

# Influence of A-site deficiency on oxygen-vacancy-related dielectric relaxation, electrical and temperature stability properties of CuO-doped NKN-based piezoelectric ceramics

Cheng-Che Tsai<sup>a,\*</sup>, Sheng-Yuan Chu<sup>b</sup>, Cheng-Shong Hong<sup>c</sup>, Song-Ling Yang<sup>b</sup>

<sup>a</sup>Department of Electronics Engineering and Computer Science, Tung Fang Design University, Kaohsiung 829, Taiwan, ROC

<sup>b</sup>Department of Electrical Engineering, National Cheng Kung University, Tainan 701, Taiwan, ROC

<sup>c</sup>Department of Electronic Engineering, National Kaohsiung Normal University, Kaohsiung 824, Taiwan, ROC

Available online 16 October 2012

## Abstract

The lead-free ceramics with composition of  $(\text{Na}_{0.5}\text{K}_{0.5})_{0.9975-x}\text{Ca}_{0.0025}\text{NbO}_3 + 1 \text{ mol\% CuO}$  (NKN–100 $x$ –C–1, where  $x=0, 0.02, 0.03, 0.04, 0.06, 0.08$ ) were synthesized by the mixed-oxide method at a sintering temperature of 1080 °C. Effects of Na and K deficiency amounts of  $x$  on the oxygen vacancies relating to the electrical and temperature stability properties were systematically investigated. Experimental results showed that the bulk densities of composition ceramics increased with increasing  $x$  contents due to the sintering aid of TTb formation at the grain boundary. The electrical properties of NKN–100 $x$ –C–1 ceramics exhibited the optimum values: bulk density  $\rho \sim 4.45 \text{ g/cm}^3$ , dielectric constant ( $\epsilon_{33}^T/\epsilon_0$ )  $\sim 255$ , dielectric loss ( $\tan\delta$ )  $\sim 0.003$ ,  $k_p \sim 0.38$ ,  $k_t \sim 0.49$ ,  $g_{33} \sim 39 \times 10^{-3} \text{ V-m/N}$ , and  $Q_m \sim 2850$ . Furthermore, the change rate of  $k_p$  and  $Q_m$  versus temperature ( $TCk_p$  and  $TCQ_m$ ) could increase by 7% and 35% in the temperature range 20–120 °C, respectively. This may be due to the decrease of mechanical damping. The imaginary part impedance of NKN–100 $x$ –C–1 ceramics with the  $x$  variation was evaluated, and the activation energy was correspondingly calculated, which disclosed the deficient  $x$  amounts correlating with the oxygen vacancy and high  $Q_m$  value.

© 2012 Elsevier Ltd and Techna Group S.r.l. All rights reserved.

**Keywords:** Non-stoichiometric composition; Oxygen vacancies; Activation energy; Arrhenius law

## 1. Introduction

Lead-free piezoelectric ceramics have attracted considerable attention as compared with PZT ceramics for the growing environmental demand. The alkaline niobate  $\text{Na}_{0.5}\text{K}_{0.5}\text{NbO}_3$  (abbreviated as NKN) ceramics is considered one of the promising candidates for the lead-free piezoelectric ceramics since the high Curie temperature (420 °C), strong ferroelectric properties and good piezoelectric properties [1,2]. However, it is difficult to obtain the dense ceramics due to Na and K volatilisation at high sintering temperature, using the mixed-oxide method. As a result, the piezoelectric properties are degraded. Hot-pressed NKN ceramics possess good piezoelectric

properties such as  $d_{33} = 160 \text{ pC/N}$ ,  $k_p = 0.45$  and achieving the relative density of 99% [3]. While this method is not suitable for mass production at low cost, the mixed-oxide method is still adopted.

Therefore, a number of studies had been carried out to improve the sintered densities and properties of NKN ceramics. These studied researches include the formation of solid solutions of NKN with other  $\text{ABO}_3$ -type ferroelectrics and non-ferroelectrics ( $A = \text{Mg, Ca, Sr, Ba, Li}$ ;  $B = \text{Ti, Sb, Ta}$ ) [2], the use of sintering aids, e.g. ZnO,  $\text{MnO}_2$ , CuO, CuO-based compound, and  $\text{K}_3\text{Li}_2\text{Nb}_5\text{O}_3$  [1,2,4]. The addition of  $\text{ABO}_3$ -type compounds to NKN-based ceramics could effectively shift the orthorhombic–tetragonal phase transition temperature ( $T_{o-t}$ ) towards room temperature, resulting in enhancing the “soft” effect. However, as the CuO, or CuO-based compound, or  $\text{K}_3\text{Li}_2\text{Nb}_5\text{O}_3$  is added to NKN ceramics system, the enhanced “hard” effect are induced, causing the higher  $Q_m$  value [5].

\*Corresponding author. Tel.: +886 7 6939626; fax: +886 7 6933406.

E-mail addresses: [jjtsai@mail.tf.edu.tw](mailto:jjtsai@mail.tf.edu.tw), [jertsai@seed.net.tw](mailto:jertsai@seed.net.tw) (C.-C. Tsai).

Recently, some literature [6,7] had reported that the excess or deficiency of A-site ion and/or B-site crystal structure in native composition could further improve the piezoelectric properties and reproducibility. In our previous works [5,7], the hard piezoelectric properties of CuO-doped NKN-based ceramics are predominately improved by using the non-stoichiometric composition or using the B-site oxide precursor method processing.

However, few papers investigate the CuO-doped deficient (Na,K) content of NKN-based ceramics on the dielectric relaxation, electrical and temperature stability properties. Therefore, an extension to our previous works is the main purpose and simultaneously investigates above-mentioned researches in correlation with hard piezoelectric properties.

## 2. Experimental procedure

The ceramic samples with the non-stoichiometric formulation of  $(\text{Na}_{0.5}\text{K}_{0.495}\text{Ca}_{0.0025})_{1-x}\text{NbO}_3 + 1 \text{ mol}\% \text{ CuO}$  (abbreviated as NKN-100x-C-1, where  $x=0, 0.02, 0.03, 0.04, 0.06$  and  $0.08$ ) were prepared by the mixed-oxide method. The pure reagents of  $\text{Na}_2\text{CO}_3$ ,  $\text{K}_2\text{CO}_3$ ,  $\text{Nb}_2\text{O}_5$ ,  $\text{CaCO}_3$  with more than 99.2% were used as the starting powders. Then, they were weighed according to the desired composition. The starting materials were transferred to a 100 mm diameter cylindrical plastic jar, partially filled with 10 mm diameter yttrium-stabilized zirconium balls and then were ball-milled for 24 h with ethanol (99.5%), followed by drying. In order to enhance the uniformity of the composition, the drying powder was calcined twice at  $900^\circ\text{C}$  in air for 5 h. Then, the proportional amount of CuO was added to the calcined powders. These compound powders were ball-milled with ethanol for 24 h again, and then were dried. The milled powders were mixed with 12 wt% PVA solution and sieved with 100 mesh, and then were uniaxially pressed into green disks with 15 mm diameter and 2 mm in thickness at a pressure of  $25 \text{ kg/cm}^2$  as samples. After burning out the PVA, the samples were placed in the setter surrounded by the same composition of packing powders and were sintered at  $1080^\circ\text{C}$  for 3 h.

Bulk densities were measured by the Archimedes method. The microstructure was observed by field emission scanning electron microscopy (FESEM) with a Hitachi S-4100 microscope. The crystallographic study was confirmed by X-ray diffraction (XRD) using  $\text{CuK}\alpha$  ( $\lambda=0.154 \text{ nm}$ ) radiation with a Siemens D-5000 diffractometer operated at 40 kV and 40 mA. To measure the electrical properties, silver paste was painted on both sides of the samples to form electrodes, and then subsequently fired at  $750^\circ\text{C}$  for 10 min. The dielectric properties of un-poled samples were measured with an impedance analyzer (HP-4192 A). Poling process was performed under a 30 kV/cm DC field at  $120^\circ\text{C}$  in silicone oil for 30 min. Then the samples were aged for 24 h. The piezoelectric properties were determined by the resonance and anti-resonance

method using an impedance analyzer (HP 4294A) according to the IEEE Standard.

## 3. Results and discussion

Fig. 1 shows the XRD patterns of NKN-100x-C-1 ceramics with  $x=0, 0.02, 0.03, 0.04, 0.06$  and  $0.08$ , sintered at  $1080^\circ\text{C}$  for 3 h. All the composition ceramics present a perovskite structure with orthorhombic symmetry. As  $x$  is above 0.06, the second phase ( $\text{K}_4\text{CuNb}_8\text{O}_{23}$ ) with tungsten bronze-type (TTB) is obviously found. It is indicated that for the small amount of alkaline deficient ( $x < 0.06$ ) samples, the diffraction peaks with coexisting tungsten bronze-type and orthorhombic structures in NKN-100x-C-1 ceramics are heavily overlapped, while as  $x > 0.06$ , the excess CuO-based compound gradually segregating at the grain boundary, the second phase is formed and the diffraction peaks are detected in the XRD patterns. This result is similar to the reported literatures [4–6]. In addition, the positions of two diffraction peaks (002) and (200) are slightly shifted to the higher angle with increasing the  $x$  contents, indicating that the crystal structure is slightly deformed and the volume is slightly decreased. Meanwhile, the bulk density of NKN-100x-C-1 ceramics increases with increasing  $x$  contents and achieves the maximum value of  $4.46 \text{ g/cm}^3$  at  $x=0.04$ , and then drops to  $4.30 \text{ g/cm}^3$  at  $x=0.08$ . This indicates that the deficiency amounts of (Na, K) results in the faster diffusion transport in the material system, which leads to the dense structure with increasing  $x$  contents up to  $x=0.04$ .

The SEM images of NKN-100x-C-1 ceramics with  $x=0, 0.02, 0.04$ , and  $0.06$  are shown in Fig. 2(a–d). They show that the grain size of NKN-100x-C-1 ceramics slightly decreases with increasing the  $x$  contents, which is similar to the results by the previous reported literature [6,7]. Simultaneously, it is demonstrated that the deficient  $x$  amounts could suppress the grain growth achieving the much more homogeneous structure and further enhance the bulk density. This attributes to the more CuO-based compound forming the liquid phase at the grain boundary inhibiting the grain growth. However, over grain growth of NKN-100x-C-1 specimens with  $x=0$  could not obtain the maximum density due to the cavities easily forming as

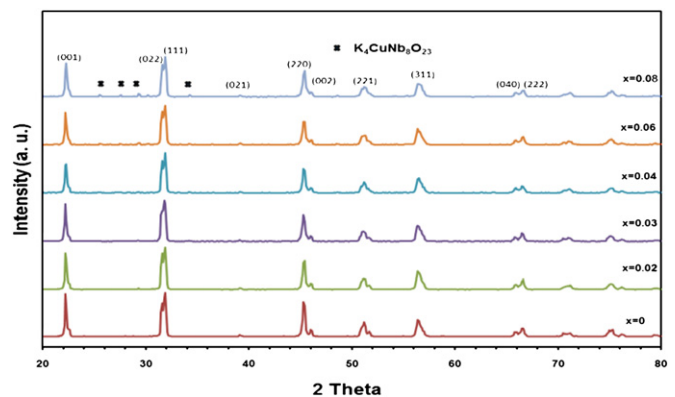


Fig. 1. XRD patterns of NKN-100x-C-1 ceramics.

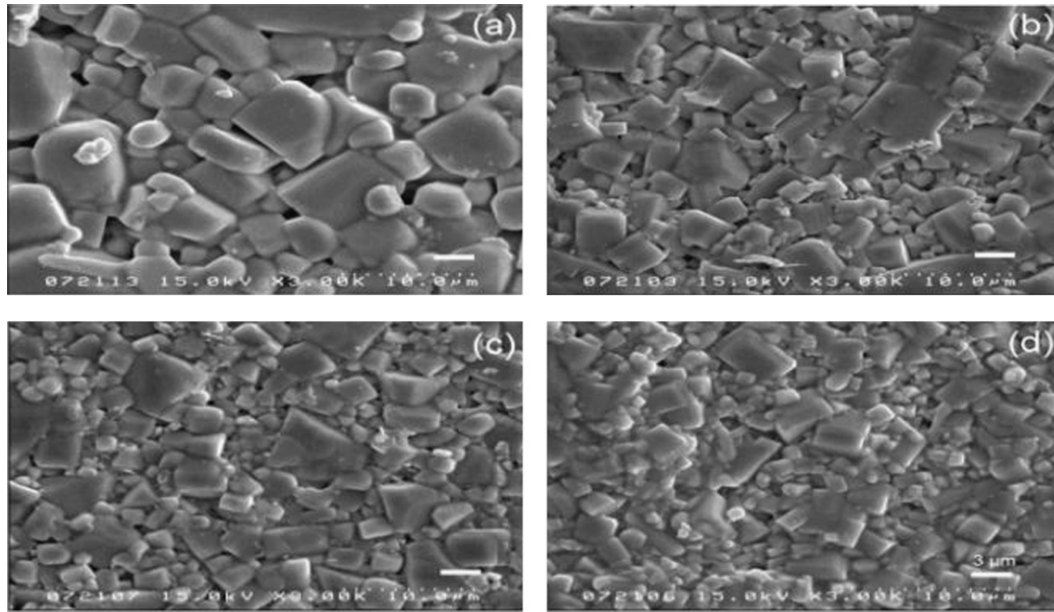


Fig. 2. SEM images of NKN-100 $x$ -C-1 ceramics (bar=3  $\mu$ m): (a)  $x=0$ , (b)  $x=0.02$ , (c)  $x=0.04$  and (d)  $x=0.06$ .

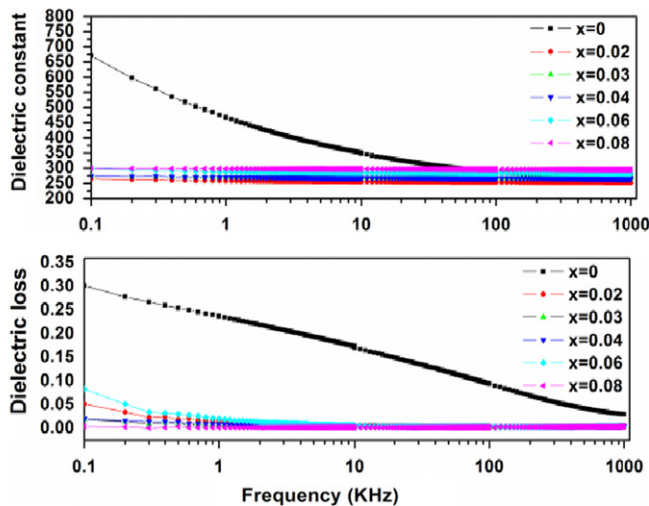


Fig. 3. Dielectric constant and loss as a function of measurement frequency at various  $x$  for NKN-100 $x$ -C-1 ceramics.

shown in SEM image observation (Fig. 2(a)). Therefore, suitable tuning the composition specimens could promote the physical properties for non-stoichiometric NKN-100 $x$ -C1 ceramics.

The dielectric constants and dielectric losses versus frequency as a function of  $x$  for NKN-100 $x$ -C-1 specimens are shown in Fig. 3. It is observed that the dielectric constant and dielectric loss decrease with increasing frequency and then saturate due to the presence of space charge, dipolar, and ionic polarizations versus measurement frequency variations in this system. In addition, the dielectric constant and dielectric loss decrease with  $x$  up to 0.06 due to the decrease of the grain size of the microstructure. Further increasing  $x$ , the dielectric loss greatly

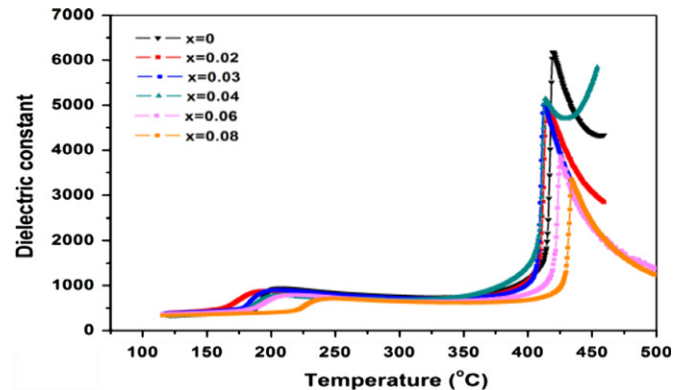


Fig. 4. Dielectric constant as a function of temperature at various  $x$  for NKN-100 $x$ -C-1 ceramics.

increases. It is attributed to the more amount of second phase ( $\text{K}_4\text{CuNb}_8\text{O}_{23}$ ) segregating at grain boundary resulting in the increase of dc conductivity due to increasing the space charge diffusion [7].

The temperature dependence of dielectric constant at a10 kHz for un-poled samples at different  $x$  contents is shown in Fig. 4. All curves present two anomalies. The first one is orthorhombic to tetragonal phase transition temperature close to 200  $^\circ\text{C}$  ( $T_{o-t}$ ) at  $x=0$  and then slightly shifts to 190  $^\circ\text{C}$  with increasing until  $x=0.02$  due to the A-site deficiency leading to the easy release of the thermal stress. Further increasing  $x$ , the  $T_{o-t}$  is toward the higher temperature due to gradual increasing the amount of second phase segregation. The second one is Curie temperature ( $T_c$ ) which presents a clear sharp peak of the dielectric constant close to 405  $^\circ\text{C}$ , corresponding to the ferroelectric tetragonal phase to paraelectric cubic phase transition. Furthermore, the  $T_c$  of NKN-100 $x$ -C-

ceramics is the same trend as the  $T_{o-t}$  with increasing  $x$  contents. And, the dielectric constants of all ceramics samples show sharp increase and no frequency dispersion near the  $T_C$ , which agree with the Debye equation [9].

The complex impedance spectroscopy (CIS) is a very convenient and powerful experimental technique, which enable us to correlate with the electrical properties of a material with its microstructure and defect content, and to analyze the dynamics of the ionic movement of the solid. From the CIS technique, the real part impedance ( $Z'$ ) and imaginary part impedance ( $Z''$ ) versus temperature and frequency are measured from the complex impedance ( $Z^*$ ) of LCR meter. The maximum dielectric relaxation time ( $\tau$ ) or frequency ( $f_{max}$ ) can be calculated by the apex of a circle in the complex plane ( $Z'$  vs.  $Z''$ ) or a Debye peak in the spectroscopy plot of  $Z''$  versus log-frequency. Fig. 5 and its inset show the  $Z'$  and  $Z''$  as a function of measurement frequency at the temperature of 390 °C, 430 °C and 460 °C (not shown in the temperature above 460 °C) for ceramics samples except  $x=0.08$ . It indicates that the all  $Z'$  values for NKN–100 $x$ –C–1 ceramics exhibit the lower frequency dispersion and a decreasing trend with increasing frequency and temperature due to the thermally assisted electric or ionic motion. However, at higher frequency, it

merges above 100 kHz independent of the frequency and the temperature. In addition, it reveals that  $Z''$  also increases with the increase of frequency and temperature and then reaches the maximum for the temperature above 380 °C. Moreover, the maximum of  $Z''$  also shifts to a higher frequency side with increasing temperature, indicating a single relaxation process from the oxygen vacancy contribution in the NKN–100 $x$ –C–1 ceramics system.

The normalized imaginary part  $Z''/Z'_{max}$  of complex impedance versus measurement frequency at the selected temperature and  $x$  content is shown in Fig. 6. It can be seen that the  $Z''/Z'_{max}$  of ceramics samples presents a symmetric peak at each temperature especially for higher temperature. The relaxation frequency ( $f_m$ ) obeys the Arrhenius law given by  $f_m = f_0 \exp(-E_a/k_B T)$  [8,9], where  $f_0$  is the pre-exponential factor,  $k_B$  is a Boltzmann constant and  $E_a$  is the activation energy. The  $E_a$  can be calculated from the slope of linear fit to  $\ln(f) - 1/T$  datum using the least square method according to above-mentioned law.

The calculated  $E_a$  for ceramics samples is listed in Table 1. It shows that the relaxation process is mainly from the oxygen vacancies contribution because the value of  $E_a$  for NKN–100 $x$ –C–1 ceramics are within 0.997–1.358 eV in

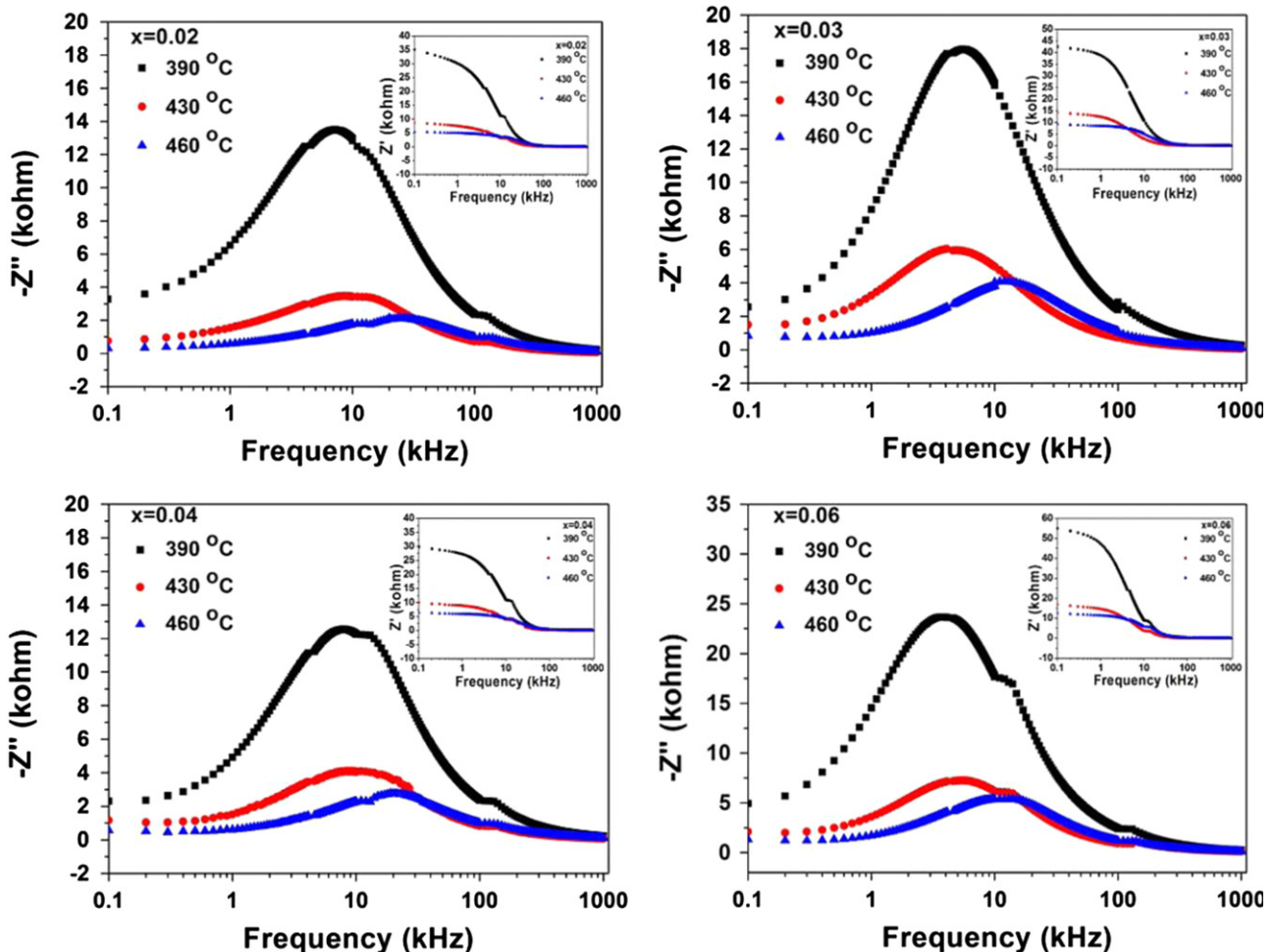


Fig. 5. Complex impedance for NKN–100 $x$ –C–1 ceramics at various temperatures of 390 °C, 430 °C and 460 °C.

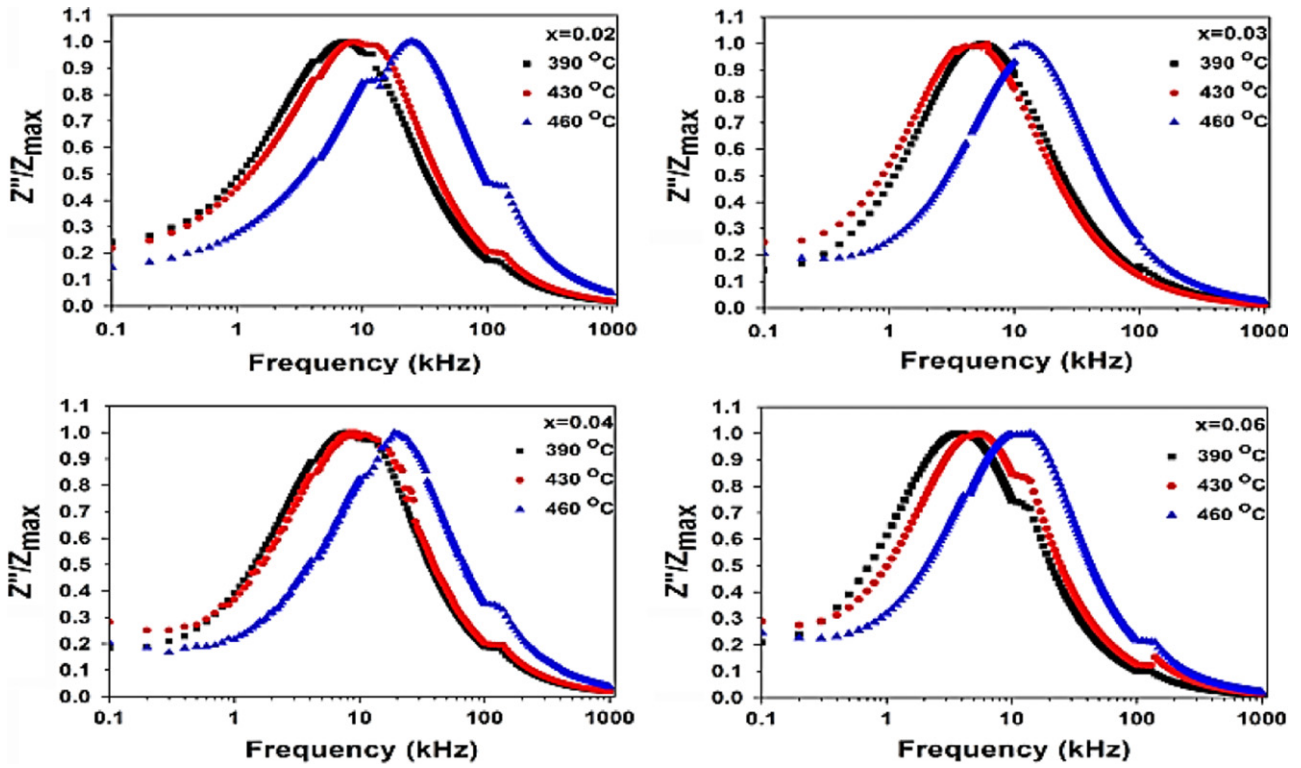


Fig. 6. Normalized imaginary part impedance of NKN–100x–C–1ceramics at temperatures of 390 °C, 430 °C, and 460 °C.

Table 1

The piezoelectric property and activation energy on relaxation frequency for NKN–100x–C–1 ceramics.

x	0	0.02	0.03	0.04	0.06
$k_p$	0.34	0.36	0.37	0.39	0.37
$Q_m$	600	1750	2850	2500	2100
$g_{33}$ (V-m/N)	0.025	0.035	0.039	0.038	0.034
$E_a$ (eV)	1.302	1.254	0.994	1.061	1.251

agreement with the reported data [8]. Table 1 also present the piezoelectric properties in the same composition samples. The optimum composition presents  $k_p$ ,  $Q_m$ ,  $g_{33}$  and  $E_a$  values of 37%, 2850,  $39 \times 10^{-3}$  V-m/N and 0.994 eV, respectively, occurred at  $x=0.03$ . Therefore, the deficient  $x$  contents in NKN–100x–C–1 ceramics can finely tune  $Q_m$ , achieving the maximum value. The obtained  $Q_m$  value in the deficient NKN-based ceramics are larger than that in the nominal CuO-doped NKN ceramics. It is attributes to the suitable adjustment in activation energy leading to the more amount of the defect dipole ( $2V_{K,Na'} - V_{O\cdot}$ ) resulting in enhancing the “hard” effect as evidenced by the CIS analysis. Thus, the induced oxygen vacancy amounts indeed play the important role in enhancing the ceramic dense and extremely high mechanical quality factor in this study.

Fig. 7 shows the temperature stability of  $k_p$  and  $Q_m$  for NKN–100x–C–1 specimens at  $x=0, 0.02, 0.03, 0.04$  and  $0.06$ . The change rate of  $k_p$  and  $Q_m$  are calculated according to our reported papers [5,7]. The change rate of  $Q_m$  value with temperatures in  $x$  range 0.02–0.06 first increased and then slightly decreased, while for  $x=0$  the

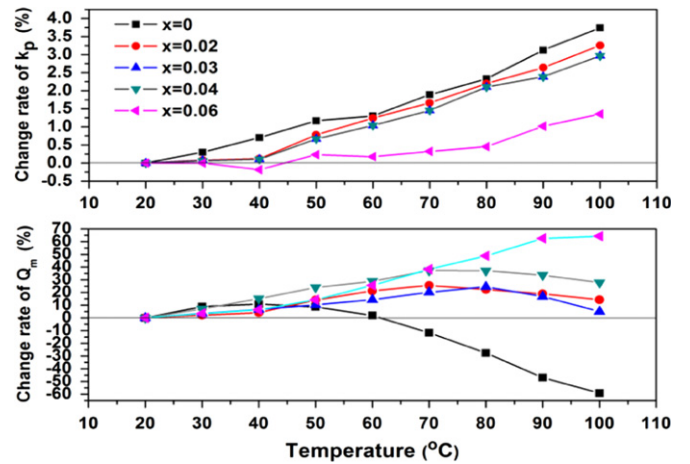


Fig. 7. The change rate of  $k_p$  and  $Q_m$  versus temperature stability of NKN–100x–C–1 ceramics in the temperature range 20–100 °C.

change rate of  $Q_m$  versus temperature presents the decreasing trend. In addition, the change rate of  $k_p$  versus temperature also shows the decreasing trend with

increasing  $x$ . It can be speculated that the change rate of  $Q_m$  with temperature is influenced by the oxygen vacancies which is correlated with the domain wall motion.

#### 4. Conclusion

The physical and electrical properties of non-stoichiometric lead-free NKN–100 $x$ –C1 ceramics with varied  $x$  deficient contents had been systematically investigated. The oxygen vacancies profoundly affect the complex impedance and activation energy, which correlate with the piezoelectric properties.

#### Acknowledgment

This work was supported from the research funding of the Hwang Sun Co. Ltd., and the technical assistance was conducted by the Acoustic and Electric-Optical Materials Lab of Department of Electrical Engineering from the National Cheng Kung University.

#### References

- [1] P.K. Panda, Review: environmental friendly lead-free piezoelectric materials, *Journal of Materials Science* 44 (2009) 5049–5062.
- [2] J. Rodel, W. Jo, K.T.P. Seifert, E.M. Anton, T. Granzow, D. Damjanovic, Perspective on the development of lead-free piezoceramics, *Journal of the American Ceramic Society* 92 (2009) 1153–1177.
- [3] R.E. Jaeger, L. Egerton, Hot pressing of potassium–sodium niobates, *Journal of the American Ceramic Society* 45 (1962) 209–213.
- [4] I.Y. Kang, I.T. Seo, Y.J. Cho, J.H. Choi, S. Nahm, T.Y. SungJ., H. Paik, Low temperature sintering of ZnO and MnO<sub>2</sub>-added (Na<sub>0.5</sub>K<sub>0.5</sub>)NbO<sub>3</sub> ceramics, *Journal of the European Ceramic Society* 32 (2012) 2381–2387.
- [5] S.L. Yang, C.C. Tsai, Y.C. Liu, C.S. Hong, B.J. Li, S.Y. Chu, Investigation of CuO-doped NKN ceramics with high mechanical quality factor synthesized by a B-site oxide, *Journal of the American Ceramic Society* 95 (2012) 1011–1017.
- [6] S.H. Moon, S.H. Han, H.W. Kang, H.G. Lee, K.W. Chae, J.S. Kim, C.I. Cheon, Crystal phase and electric properties of (Na<sub>0.5</sub>K<sub>0.5</sub>)<sub>1-x</sub>Nb<sub>1+x/5</sub>·yCuO, zLiSbO<sub>3</sub> piezoceramics, *Ceramics International* 38S (2012) S343–S346.
- [7] C.C. Tsai, S.F. Chen, S.Y. Chu, C.M. Cheng, M.C. Kung, The characteristics of ultrasonic therapeutic transducers and used lead-free non-stoichiometric NKN-based piezoelectric ceramics, *Current Applied Physics* 11 (2011) S128–S133.
- [8] L. Liu, H. Fan, L. Fang, X. Chen, H. Dammak, M.P. Thi, Effects of Na/K evaporation on electrical properties and intrinsic defects in Na<sub>0.5</sub>K<sub>0.5</sub>NbO<sub>3</sub> ceramics, *Materials Chemistry and Physics* 117 (2009) 138–141.
- [9] G. Singh, V.S. Tiwari, P.K. Gupta, Role of oxygen vacancies and conduction behaviour of KNbO<sub>3</sub>, *Journal of Applied Physics* 107 (2010) 064103.